JOURNAL OF GEOPHYSICAL RESEARCH, VOL. 102, NO. D24, PAGES 29,429–29,443, DECEMBER 26, 1997

Leaf area index of boreal forests: Theory, techniques, and measurements

Jing M. Chen,[1] Paul M. Rich,[2] Stith T. Gower,[3] John M. Norman,[4] and Steven Plummer[5]

Abstract. Leaf area index (LAI) is a key structural characteristic of forest ecosystems because of the role of green leaves in controlling many biological and physical processes in plant canopies. Accurate LAI estimates are required in studies of ecophysiology, atmosphere-ecosystem interactions, and global change. The objective of this paper is to evaluate LAI values obtained by several research teams using different methods for a broad spectrum of boreal forest types in support of the international Boreal Ecosystem-Atmosphere Study (BOREAS). These methods include destructive sampling and optical instruments: the tracing radiation and architecture of canopies (TRAC), the LAI-2000 plant canopy analyzer, hemispherical photography, and the Sunfleck Ceptometer. The latter three calculate LAI from measured radiation transmittance (gap fraction) using inversion models that assume a random spatial distribution of leaves. It is shown that these instruments underestimate LAI of boreal forest stands where the foliage is clumped. The TRAC quantifies the clumping effect by measuring the canopy gap size distribution. For deciduous stands the clumping index measured from TRAC includes the clumping effect at all scales, but for conifer stands it only resolves the clumping effect at scales larger than the shoot (the basic collection of needles). To determine foliage clumping within conifer shoots, a video camera and rotational light table system was used. The major difficulties in determining the surface area of small conifer needles have been largely overcome by the use of an accurate volume displacement method. Hemispherical photography has the advantage that it also provides a permanent image record of the canopies. Typically, LAI falls in the range from 1 to 4 for jack pine and aspen forests and from 1 to 6 for black spruce. Our comparative studies provide the most comprehensive set of LAI estimates available for boreal forests and demonstrate that optical techniques, combined with limited direct foliage sampling, can be used to obtain quick and accurate LAI measurements.

1. Introduction

The boreal forest is the second largest biome, and there is increasing interest in this biome for its role in the terrestial carbon cycle. One key to characterizing forest stands is obtaining accurate and meaningful measures of the forest canopy. Leaf area index (LAI) is one of the primary measures used in remote sensing and process-based models to characterize plant canopies [Sellers *et al.,* 1986; *Running and Coughlan*, *1988; Bonan,* 1993]. LAI estimates are used for two basic purposes: (1) as an ecophysiological measure of the photosynthetic and transpirational surface within a canopy, and (2) as a remote sensing measure of the leaf reflective surface within a canopy. While excellent measurements of LAI have been made for small-stature vegetation such as agricultural crops and plantations, measurements for natural ecosystems such as boreal forests have proven more difficult. Measurements for boreal forests are particularly challenging to obtain because of inherent difficulties in making direct measurements of forests, high levels of natural variability, lack of standards, difficulty of distinguishing leaf area from wood tissue, and difficulty of generalizing local measurements to a landscape scale. The international Boreal Ecosystem-Atmosphere Study (BOREAS), which seeks to understand the role of boreal forests in global climate, has served as an impetus to collect comprehensive measurements of LAI for boreal forests and to compare the various LAI measurement techniques.

The major methodologies for estimating LAI employ either "direct" measures (involving destructive sampling, litterfall collection, or point contact sampling) or "indirect" methods (involving optical instruments and models). Direct destructive sampling methods have been used successfully in agricultural systems but must depend upon extrapolation using allometric methods for forest systems. Litterfall collection is useful for deciduous forests with adequate spatial and temporal sampling schemes *[Neumann et al.,* 1989], but this methodology is not useful for evergreen forests because the needle fall in a year is directly related to neither the new growth in the year nor the growth in the previous year, but rather to the average life span of needles and the cumulative climate conditions over the life span. The point contact method [*Warren-Wilson*, 1965], which

[1]Applications Division, Canada Centre for Remote Sensing, Ottawa, Ontario.
[2]Department of Systematics and Ecology, Kansas Biological Survey and Environmental Studies Program, University of Kansas, Lawrence.
[3]Department of Forestry, University of Wisconsin, Madison.
[4]Department of Soil Science, University of Wisconsin, Madison.
[5]British National Space Centre, Abbots, Ripton, Huntingdon, Cambridgeshire, England.

Paper number 97JD01107.
0148-0227/97/97JD-01107$09.00

determines LAI from the mean contact number of a thin probe that passes through the canopy, is impractical in forest stands because of the tall stature of trees and the high density of conifer leaves. By contrast, indirect optical methods hold great promise because of the potential to obtain quick and low-cost measurements over large areas. However, several commercial optical instruments, including the LAI-2000 plant canopy analyzer (LI-COR, Lincoln, Nebraska) and Sunfleck Ceptometer (Decagon Devices, Pullman, Washington), are hindered by the complexity of canopy architecture in natural forest stands. Therefore much effort is needed to improve the indirect techniques.

Canopy architecture may be separated into two essential attributes: foliage angle distribution and foliage spatial distribution. The commercial instruments and hemispherical photograph techniques are well suited for measuring LAI without a priori knowledge on the leaf angle distribution by acquiring multiple angle gap fraction data [*Welles*, 1990], but estimates of LAI, especially for conifers, are often incorrect because foliage spatial distribution is not random, a key assumption to gap fraction models. Violation of this assumption is most serious for boreal forests which have open canopies where tree crown, branch, and shoot structures dictate the spatial distribution of leaves, making it nonrandom (clumped). *Chen and Cihlar* [1995a] developed an optical instrument named TRAC (tracing radiation and architecture of canopies) and theory to measure LAI of clumped canopies. The theory utilizes canopy gap size information in addition to canopy gap fraction and provides a foliage clumping index which quantifies the effect of nonrandom spatial distribution of foliage on LAI measurements. Gap size refers to the dimension of a gap, while gap fraction can be defined as the percentage of sky seen from beneath the canopy. For the same gap fraction, there can be different gap size distributions. The TRAC and its theory have been tested in conifer stands in eastern Canada using direct LAI measurements *[Chen and Cihlar,* 1995a] and applied to several BOREAS conifer sites without further validation *[Chen and Cihlar,* 1995b].

Hemispherical (fish-eye) canopy photography is a technique for characterizing plant canopies using photographs taken looking upward through an extreme wide-angle lens *[Evans and Coombe,* 1959; *Anderson,* 1964; *Bonhomme et al., 1974; Pearcy*, 1989; *Rich,* 1990; *Chen et al.,* 1991; *Galo et al.,* 1992; *Lin et al.,* 1992; *Lerdau et al.,* 1992; *Mitchell and Whitmore*, 1993; *Clark et al.,* 1996]. The geometric distribution of openings can be measured precisely and used to estimate solar radiation interception *[Rich et al.,* 1993] and to estimate aspects of canopy architecture such as LAI and leaf angle distribution. The LAI-2000 may be regarded as a convenient version of hemispherical photography because image processing is not required, but the latter has various advantages: (1) it is capable of reducing the blue light scattering effect by correctly setting the threshold value to distinguish grey foliage from sky; (2) it acquires permanent digital images of the canopy, which allows visual examination of the canopy features; and (3) the hemispheric image can be divided into desired numbers of rings to improve the calculation of LAI and into sections to investigate the azimuthal distribution of foliage. The Sunfleck Ceptometer can be used to measure the average transmittance of direct solar radiation. The transmittance can be taken as the gap fraction at the solar zenith angle. With an assumed leaf angle distribution, the transmittance at one angle can provide an estimate of LAI for the stand. However, if data are collected over half a clear day, the LAI can be calculated without such an assumption. If the direct and diffuse radiation are separated, the instrument also has the advantage of reducing the scattering effect. The instrument can also be used to remove the effect of large-scale clumping on LAI measurements when the finite averaging length method *[Lang and Xiang*, 1986] is used. However, all of the above instruments cannot distinguish foliage from wood tissue, and the current theory used by scientists to calculate LAI from gap fraction measurements assumes random distribution of foliage elements.

This paper has three objectives: (1) to evaluate different methodologies for measuring LAI in forest ecosystems, including the major optical techniques (LAI-2000, TRAC, Ceptometer, and hemispherical photography) and labor-intensive destructive sampling; (2) to test new theories and techniques to quantify the effect of foliage clumping at various scales on LAI estimates; and (3) to provide LAI estimates for a broad spectrum of boreal forest stands, in particular all the BOREAS tower flux sites and some auxiliary sites.

2. Theory

2.1. Definition of LAI

The definition of LAI used in this paper is one half the total green leaf area per unit ground surface area. This definition was first proposed by *Chen and Black* [1992a] and agrees in principle with the independent and simultaneous work of *Lang* [1991]. This definition has been used by *Fassnacht et al.* [1994] and is the same as that used by *Stenburg et al.* [1994]. The major advantage of the new definition over the definition based on the projected (one-sided) area *[Ross,* 1981] is that when the foliage angular distribution is spherical (random), the usual projection coefficient of 0.5 can still be used for objects of any shape. Since foliage elements are oriented in various directions in plant canopies, the projected area in one direction does not contain all the information for estimating radiation interception. The use of half the total area, which in effect, is twice the average projected area for all leaf inclination angles, avoids this problem.

2.2. Definition of Effective LAI

Many optical instruments measure canopy gap fraction based on radiation transmission through the canopy. Assuming a random spatial distribution of leaves, the effective LAI *(L,)* can be calculated from the gap fraction by adopting *Miller's* [1967] theorem summarized in the following equation:

$$L_e = 2 \int_0^{\pi/2} \ln \left[\frac{1}{P(\theta)} \right] \cos \theta \sin \theta \, d\theta \qquad (1)$$

where $P(\theta)$ is the gap fraction at the view zenith angle. Although this equation was originally developed for the calculation of LAI, *Chen et al.* [1991] regard the result from (1) as the effective LAI because leaves in plant canopies are often not randomly distributed in space. The meaning of this term is perhaps better understood with the following expression [*Nilson,* 1971]:

$$P(8) = \exp \left[-G(\theta) \Omega L_t / \cos (\theta) \right] \qquad (2)$$

where $G(\theta)$ is the projection coefficient characterizing the foliage angle distribution, L_t is the plant area index including leaf and woody areas, and Ω is a parameter determined by the

spatial distribution pattern of leaves. When the foliage spatial distribution is random, Ω is unity. If leaves are regularly distributed (extreme case: leaves are all laid side by side), Ω is larger than unity. When leaves are clumped (extreme case: leaves are stacked on top of each other), Ω is less than unity. Foliage in plant canopies is generally clumped, and hence Ω is often referred to as the clumping index. With multiple angle measurements of *P(6), G(8)* and ΩL_t can be computed simultaneously *[Norman and Campbell,* 1989]. Without the knowledge of Ω, only the product of Ω and L_t can be obtained from gap fraction measurements. Since ΩL_t is an important quantity determining the canopy gap fraction and hence the radiation environment in the canopy, it deserves the separate term "effective LAI," denoted by L_e.

An important consideration implicitly expressed in (1) is that LAI can be calculated without knowledge of foliage angle distribution if the gap fraction is measured at several zenith angles covering the full range from 0 to $\pi/2$. The LI-COR LAI-2000 is well suited for this purpose because of its ability to measure $P(\theta)$ at five zenith angles simultaneously from diffuse blue light transmission through the canopy. Hemispherical photography can also provide gap fractions in the full zenith angle range and hence can be used to measure L_e.

2.3. Deriving LAI From L_e

Since L_e is obtained from gap fraction measurements and is the quantity that many optical instruments measure, *Chen* [1996a] used it as a basis for calculating LAI using the following equation:

$$L = (1 - \alpha) L_e / \Omega \tag{3}$$

where α is the woody-to-total area ratio. Since L_e is usually measured near the ground surface based on radiation transmission, all aboveground materials, including green and dead leaves, branches, and tree trunks and their attachments (lichen, moss), intercept light and are included in L_e. By using the factor $(1 - \alpha)$, the contributions of nonleafy materials are removed. However, the removal using this simple parameter assumes nonwoody materials have a spatial distribution pattern similar to that of leaves quantified by St. This assumption may result in a small error in the LAI estimation. The value of a in this study is obtained through labor-intensive destructive sampling *[Chen,* 1996a]. New ways of estimating a are being investigated using a two-band camera *[Kucharik et al.,* this issue]. By (3), the remaining task in obtaining LAI is to determine Ω.

Conifer needles are grouped at several levels: shoots, branches, whirls and tree crowns, and even groups of trees. Conifer shoots (the basic collection of needles distributed around the smallest stem) are treated as the basic foliage units affecting radiation transmission *[Norman and Jarvis*, 1975; *Ross et al.,* 1986; *Oker-Blom*, 1986; *Leverenz and Hinckley, 1990; Gower and Norman,* 1990; *Fassnacht et al.,* 1994]. *Chen and Black* [1992b] and *Chen and Cihlar* [1995a] determined from canopy gap size distributions that the size of the basic foliage unit is the average projected shoot width. This is because small gaps disappear in the shadow in a short distance as a result of the penumbral effect. Therefore it is difficult to measure the amount of needle area within the shoots with optical instruments, and the Ω value has to be separated into two components as follows *[Chen,* 1996a]:

$$\Omega = \Omega_E / \gamma_E \tag{4}$$

where γ_E is the needle-to-shoot area ratio quantifying the effect of foliage clumping within a shoot (it increases with increasing clumping) and Ω_E includes the effect of foliage clumping at scales larger than the shoot (it decreases with increasing clumping). The definitions of these two terms are given in the following sections. The final equation for LAI then becomes

$$L = (1 - \alpha) L_e \gamma_E / \Omega_E \tag{5}$$

2.3.1. Foliage clumping within conifer shoots. The needle-to-shoot area ratio is used to quantify foliage clumping within shoots. *Fassnacht et al.* [1994] proposed an equation for calculating the shoot area, which is an improvement over the method of *Gower and Norman* [1990]. *Chen* [1996a] developed the following equation to calculate one half of the total shoot area *(A,),* which differs slightly from *Fassnacht et al.* [1994]:

$$A_s = \frac{1}{\pi} \int_0^{2\pi} d\Phi \int_0^{\pi/2} A_p(\theta, \Phi) \cos\theta \, d\theta \tag{6}$$

where θ is the zenith angle of projection relative to the shoot main axis and Φ is the azimuthal angle difference between the projection and the shoot main axis. A shoot having an equal projected area at all angles of projection can be approximated by a sphere. In such a case A_n, half the total shoot imaginary surface area, equals 2 times the projected area. If one half of the total area (all sides) of needles in a shoot is A_n, then

$$\gamma_E = A_n / A_s \tag{7}$$

For deciduous forests, individual leaves are considered as the foliage elements, and $\gamma_E = 1$.

2.3.2. Foliage clumping at scales larger than the shoots. The effect of foliage clumping at scales larger than the shoot is considered using Ω_E. If shoots are randomly distributed in space, Ω_E equals unity, and the γ_E correction is sufficient. For most plant canopies, foliage elements are clumped, resulting in Ω_E smaller than unity. When foliage elements are grouped at higher levels, the total gap fraction increases for the same LAI, and so does the probability of observing large gaps. A canopy gap size distribution can therefore be used to quantify Ω_E. The TRAC is designed to acquire the gap size distribution through measurements of sunfleck width along transects beneath the canopy. The theory and methods are fully described by *Chen and Cihlar* [1995a, b]. The final equation for calculating Ω_E is

$$\Omega_E = \frac{[1 + F_m(0) - F_{mr}(0)] \ln [F_m(0)]}{\ln [F_{mr}(0)]} \tag{8}$$

where $F_m(0)$ is the measured total canopy gap fraction and $F_{mr}(0)$ is the gap fraction for a canopy with randomly positioned elements. While $F_m(0)$ can be measured as the transmittance of direct or diffuse radiation at the zenith angle of interest, $F_{mr}(0)$ is obtained through processing a canopy gap size accumulation curve, *F,(h),* which is the accumulated gap fraction resulting from gaps with size A larger than or equal to λ. At $\lambda = 0$, $F_m(\lambda)$ is the total gap fraction as measured by other optical instruments. *F,(h)* can be measured by the TRAC. According to *Miller and Norman* [1971], the pattern of gap size accumulation for a random canopy, denoted by *F,(h),* can be predicted from LAI and the foliage element width. By comparing *F,(h)* with *F,(h),* large gaps appearing at probabilities larger than the prediction of *F,(A)* can be identified and removed from the total gap accumulation. *F,,(h)* is

$F_r(h)$ brought to the closest agreement with $F_r(X)$, representing the case of a random canopy with the same LAI. In the calculation of $F_r(\lambda)$, LAI is required, but it is unknown. *Chen and Cihlar* [1995a] solved the problem by using an iteration method. For a given measured $F_m(\lambda)$, the iteration always converges to a unique value.

2.4. Finite-Length Averaging Method

Recognizing the difficulty of measuring LAI in discontinuous canopies, *Lang and Xiang* [1986] developed a finite-length averaging method. In this method, LAI values are first calculated from many small transect measurements of gap fraction, and then the individual transect LAI values are averaged to obtain the mean stand LAI. The transect length is chosen to be 10 times the average leaf width to ensure that the statistical error is smaller than 5%. The calculation of LAI in the small transects assumes random leaf spatial distribution within each transect. *Chen and Black* [1992b] pointed out that Lang and Xiang's method has the merit of eliminating the effect of foliage clumping at scales larger than the transect, but the clumping effect at scales smaller than the transect remains. In conifer stands with small needle leaves, an additional problem exists: the required transect is too small to use because in many small locations under the canopy the direct beam transmission is zero, resulting in infinite LAI values in the inversion. To avoid the problem, we chose the length of the Sunfleck Ceptometer (Decagon Devices, Pullman, Washington, model SF-SO), 800 mm, as the finite transect length. We realize that this method can considerably underestimate LAI because of the foliage clumping within the finite length of optical measurements. If the canopy is assumed to be made up of elements that are randomly distributed within the finite measuring length (or area) and evenly distributed in azimuth with a spherical leaf angle distribution then empirical relationships can be established between the L and the transmitted photosynthetically active radiation (PAR) fraction measured by the Ceptometer at one solar zenith angle. *Norman* [1988], for example, devised the following relationship between the plant area index L_t and natural logarithm of the PAR transmittance using a radiative transfer model:

$$L_t = \frac{[f_b(1 - \cos\theta) - 1] \ln (E_i/E_a)}{0.72 - 0.337\, f_b}. \quad (9)$$

where E_a is the total incident PAR above the canopy, E_i is incident PAR beneath the canopy, θ is the solar zenith angle, and the beam fraction f_b is

$$f_b = \frac{E_a - E_{ad}}{E_a} \quad (10)$$

where E_{ad} is the diffuse PAR irradiance above the stand. This equation provides an estimate of plant area index rather than LAI because the Ceptometer measurements beneath the canopy are affected by all materials above it, including the foliage and the supporting woody materials.

2.5. Dimension Analysis or Allometry

Allometry, the relationship between a dependent variable such as size, shape, or area and an independent variable, is commonly used as a tool to directly estimate the area of tree parts. The form of the relationship varies but often follows the form log Y = a + b log X, where a and b are the Y intercept and slope of the equation, respectively, and log is the natural or lo-based logarithmic transformation needed to correct nonhomogeneous variance of the dependent variable. Allometric relationships can be obtained by destructively sampling trees and determining the biomass and area of various components, or they can be obtained from other studies. However, the application of "generalized" allometric relationships can lead to large errors, especially for foliage mass and area components [Crier et *al.,* 1984]. Allometric equations can be used to scale tree-level estimates of leaf area to the stand-level by measuring the diameter and species of all trees in a plot of known area and applying the appropriate allometric equations. While leaf area estimates for forests are common, few attempts have been made to assess the sources of errors related to direct LAI estimates. The most notable errors include (1) estimation of the foliage area:mass ratio used to convert foliage mass of a tree to area, (2) variance of the dependent variable (i.e., leaf area) around the regression equations, and (3) variance of stem density in the stand.

Using an allometric relationship to estimate the leaf area of stands has several advantages over indirect optical methods. Allometric relations enable scientists to quantify stem, branch, and foliage area separately, they allow scientists to characterize the vertical distribution of LAI and partition LAI by each age-cohort of foliage, and allometric equations do not require estimates of clumping factors *[Gower and Norman,* 1990; *Fassnacht et al.,* 1994; *Chen and Cihlar,* 1995a]. Disadvantages of using allometric relationships to estimate leaf area include the facts that (1) they are time consuming and expensive to develop, (2) numerous abiotic and biotic factors influence the allometric relations, thereby necessitating site-specific allometric equations, and (3) destructive analysis of trees may not be permitted in wilderness areas or parks.

3. Methods

3.1. Study Sites

Study sites are located in forest stands of major boreal species: black spruce (*Picea mariana),* jack pine (*Pinus banksiana),* and aspen (*Populus tremuloides),* located in the BOREAS southern study area (SSA) near Prince Albert and Candle Lake, Saskatchewan, and in the northern study area (NSA) near Thompson and Nelson House, Manitoba. Table 1 provides a list of stand attributes for the sites investigated, where SOBS, SOJP, SYJP, and SOA denote the old black spruce, old jack pine, young jack pine, and old aspen sites in the SSA, respectively, and likewise, NOBS, NOJP, and NYJP in the NSA. These are sites with an eddy covariance tower and are considered to be the intensive sites. NOA is an auxiliary site. Other five letter/digit names (Table 2) are auxiliary sites of BOREAS (i.e., these sites did not have the eddy covariance tower).

LAI was measured every 10 m, marked by permanent flags, along three transects (A, B, and C) with the B transect passing next to the eddy covariance tower along the edge of the wind-aligned blob (WAB) centered at the tower (Figure 1). The mapped plot for hemispherical photograph acquisition overlaid part of the transects. All transects in the intensive sites except for SOA were oriented in the SE-NW direction. In SOA the transects extended SW from the tower 300 m. In SOBS, SOJP, NOBS, and NOJP, the NW end of the B transect was the tower, while in SYJP and NYJP the tower was located at the center of the B transect, i.e., the transects traversed from the SE to the NW part of the WAB. The allometry plots used

Table 1. Site Description

Stand	Age, years	Tree Height, m	Density, stems/ha	Latitude, °N	Longitude, °W	Transect, m
SOJP	60-75	12-15	1600-4000	53.916	104.692	200
SYJP	11-16	4-5	4000-4100	53.877	104.647	300
SOBS	o-155	O-10	3700-5800	53.987	105.122	300
SOA	60	21	900	53.627	106.194	300
NOJP	50-65	9-13.5	1300-3500	55.928	98.624	210
NYJP	25	O-2.5	5700–42,000	55.905	98.288	340
NOBS	75-90	9-12	1150-8700	55.880	98.484	300
NOA				55.532	98.405	50

Stand abbreviations are defined in the text.

for destructive sampling were generally located in the east sector outside of the WAB. At an auxiliary site, two perpendicular 50 m transects oriented in due S-N and E-W directions were used to sample LAI.

3.2. LAI-2000 and TRAC Measurement Procedures

LAI-2000 measures the transmitted blue sky light (400-490 nm) under the canopy in five concentric rings from 0° to 75°, from which to calculate the gap fraction for five zenith angle ranges and therefore the L_e using (1). LAI-2000 measurements were made at each flag position, and the mean value of L_e for a site each time was thus obtained from 60-102 measurements. Three LAI-2000 units were used in most stands: two for in-stand measurements and one for the reference measurements on remote mode either on top of the flux tower or in a nearby clearing. Data were acquired in the following BOREAS intensive field campaigns (IFCs): IFC-93 (August 9–29, 1993), IFC-1 (May 5 to June 16, 1994), IFC-2 (July 19 to August 8, 1994), and IFC-3 (August 30 to September 19, 1994). LAI-2000 measurements were made at the auxilary sites only during IFC-2 or IFC-3 at 11 locations along both of the 50 m transects. All measurements were made near sunset or under overcast conditions to reduce the effect of scattered blue light in the canopy.

The TRAC instrument consists of three PAR (400-700 nm) sensors (LI-COR, Lincoln, Nebraska, model LI-190SB), a data logger (Campbell Scientific, Logan, Utah, model CR10), and a storage module (model SM 716). With a walking pace of 1 m per 3 s at a sampling frequency of 32 Hz, the measurement interval for each sensor is about 10 mm. The transmitted total and diffuse PAR irradiance from the two upward facing sensors are used to resolve the direct component of PAR for LAI calculations, and the reflected PAR irradiance from the downward facing sensor is useful in calculating the fraction of PAR absorbed by the canopy. In making measurements, the operator needs to watch a level indicator and a shadow strip on the diffuse PAR sensor while walking at a reasonably constant speed. To minimize the effect of the operator's shadow and avoid sampling along long tree shadows or sunflecks, the measurement time was chosen to allow the difference between the transect direction and the solar azimuth angle to be larger than 30°. TRAC measurements were generally made on B transect several times at each intensive site in IFC-1, -2, and -3. In auxiliary sites, TRAC was used in IFC-3 on one or both of the transects. All TRAC measurements were made under clear-sky conditions or in large gaps between clouds, allowing uninterrupted operation for the whole transect.

3.3. Ceptometer Measurement Procedures

During IFC-2, a Sunfleck Ceptometer was used to measure total incident PAR, diffuse incident PAR, total PAR transmitted through the canopy,, and diffuse PAR in the canopy for a number of jack pine auxiliary sites located within the BOREAS SSA. At each of these sites, measurements were taken at the same 10 sampling positions used for hemispherical photography. Each PAR measurement consisted of an average of 80 PAR photodiodes in the Ceptometer for eight azimuthal orientations. Thus each site measurement constituted the average of 6400 individual measurements of PAR. Unlike the LAI-2000, a line quantum sensor measures incoming PAR over a restricted zenith range. To calculate the plant area index (PAI) without. reference to an assumed leaf angle distribution, measurements were obtained at several solar zenith angles. PA1 was calculated using (9) and the site PA1 calculated as the average of these individual estimates.

3.4. Hemispherical Photography Methods

Hemispherical photographs were acquired in sample arrays at heights of 0.8, 1.5, and 2.5 m for each of the forested BOREAS tower flux sites and auxiliary sites. For the forested tower flux sites and other sites for which mapped plots were set up, hemispherical photographs were acquired during IFC-1 and IFC-2 at 10 m intervals along the central X axis of the mapped plot (5 m intervals for NSA-YJP). Typically, this corresponds to six sample locations for each tower flux site. Site locations in relation to the flux tower (Figure 1) are SOBS, 150-230 m (SE); SOJP, 130-180 m (SE); SYJP, 30-80 m (SE); SOA, 70-120 m (SW); NOBS, 80-130 m (SE); NOJP, 70-120 m (SE); and NYJP, 120-150 m (SE). Location refers to distance from the flux tower along the "B" LAI transect, except in the case of SOBS, where a "D" line (20 m from the C line) is used. For the auxiliary sites, hemispherical photographs were taken in a crisscross array, at 10 m intervals along two 40 m long transects placed at right angles and crossing in the middle. A total of nine sample locations were chosen within the plot. The auxiliary site photographs were taken during and between IFC-1 and IFC-2.

Hemispherical photograph negatives were video digitized at a resolution of 512 (horizontal) *X* 480 (vertical) *X* 7 bits using the hemispherical photograph analysis system CANOPY *[Rich,* 1989, 1990]. Gap fraction, the proportion of unobstructed sky, was calculated at 5° zenith angle intervals and used for additional calculations. All hemispherical photographs were also archived in Kodak PhotoCD format. The effective LAI and other canopy indices were calculated using

Table 2. Mean L_e and FIPAR Values for BOREAS Auxiliary Sites

Stand, Age	Productivity	Photo Date in 1994	n	L_e Mean	L_e s.d.	FIPAR Diffuse Mean	FIPAR Diffuse s.d.	FIPAR Direct Mean	FIPAR Direct s.d.	Site
				NSA Aspen						
Disturbed	Medium	July 31	9	1.50	0.19	0.66	0.04	0.75	0.06	T8S4A
Intermediate	Low	July 4	8	2.47	0.48	0.75	0.08	0.84	0.07	T4U5A
Intermediate	Low	July 24	9	2.45	0.44	0.77	0.04	0.83	0.08	V5X7A
Intermediate	Low	July 24	9	1.72	0.28	0.64	0.07	0.71	0.06	W0Y5A
Intermediate	Medium	July 4	9	2.65	0.33	0.80	0.04	0.85	0.05	S9P3A
Mature	Medium	Aug. 4		1.90	0.32	0.74	0.07	0.84	0.06	Q3V3A
Mature	Medium	Aug. 6	9	2.66	0.45	0.79	0.07	0.85	0.04	R8V8A
Mature	High	July 4	9	1.94	0.39	0.70	0.07	0.75	0.07	T2Q6A
Mature	High	July 29	9	2.07	0.30	0.77	0.06	0.81	0.05	P7V1A
				SSA Aspen						
Disturbed	High	July 20		3.00	0.52	0.88	0.03	0.92	0.03	D6H4A
Disturbed	High	Aug. 17	9	1.68	0.20	0.62	0.04	0.71	0.03	D6L9A
Intermediate	Medium	July 27	9	2.04	0.22	0.77	0.06	0.85	0.07	B9B7A
Mature	High	June 25	9	2.93	0.28	0.84	0.02	0.86	0.04	D9G4A
Mature	High	Aug. 12	6	1.27	0.28	0.59	0.08	0.63	0.12	E7C3A
				NSA Black Spruce						
Disturbed	Low	Aug. 3	9	0.33	0.15	0.25	0.09	0.34	0.08	T7R9S
Disturbed	Medium	July 24		0.31	0.27	0.21	0.13	0.29	0.16	U6W5S
Intermediate	Low	Aug. 5	8	1.63	0.23	0.68	0.06	0.84	0.05	T3U9S
Intermediate	Medium	June 29		2.37	0.33	0.80	0.04	0.87	0.05	T4U8S
Intermediate	High	June 16	9	2.30	0.48	0.78	0.06	0.87	0.04	T6R5S
Mature	Low	July 4	10	1.58	0.38	0.62	0.09	0.74	0.08	T0P7S
Mature	Medium	June 22	9	2.53	0.15	0.81	0.02	0.89	0.03	S8W0S
Mature	Medium	Aug. 5	9	2.90	0.21	0.80	0.02	0.87	0.04	T0W1S
Mature	High	July 4	9	2.98	0.34	0.80	0.03	0.87	0.05	T0P8S
Mature	High	July 26	9	2.76	0.54	0.79	0.04	0.86	0.04	T5Q7S
				SSA Black Spruce						
Disturbed	Medium	July 26		1.31	0.37	0.60	0.08	0.69	0.13	H1E4S
Intermediate	High	July 14		3.13	0.49	0.81	0.04	0.90	6.04	G2I4S
Mature	Low	July 27		3.25	0.30	0.85	0.03	0.91	0.04	D0H6S
Mature	Low	July 30	9	3.45	0.58	0.87	0.03	0.92	0.03	G9I4S
Mature	Low	Aug. 11	8	0.23	0.11	0.19	0.07	0.25	0.09	G2L7S
Mature	Medium	Aug. 13	9	2.26	0.26	0.72	0.04	0.80	0.04	H2D1S
Mature	High	July 31	9	2.13	0.17	0.76	0.02	0.79	0.02	G6K8S
				NSA Jack Pine						
Disturbed	LOW	July 30	9	*0.80*	0.21	0.42	0.08	0.50	0.09	T8S9P
Intermediate	Low	July 25	9	1.07	0.14	0.54	0.06	0.55	0.09	T9Q8P
Intermediate	Medium	July 28		1.55	0.20	0.63	0.04	0.75	0.08	T8Q9P
Intermediate	Medium	Aug. 3	9	2.53	0.66	0.77	0.07	0.84	0.09	T7S9P
Mature	Low	July 4		0.77	0.21	0.43	0.08	0.52	0.13	O9P
Mature	High	Aug. 4		1.95	0.20	0.76	0.04	0.84	0.05	Q3V3P
				SSA Jack Pine.						
Disturbed	Medium	Aug. 3	9	1.09	0.47	0.53	0.22	0.54	0.20	G8L6P
Intermediate	Low	July 14	8	4.10	0.52	0.87	0.03	0.92	0.05	I2I8P
Intermediate	Low	July 28	9	1.95	0.20	0.69	0.03	0.76	0.06	F5I6P
Mature	Low	June 19	10	2.06	0.33	0.72	0.07	0.74	0.08	G4K8P
Mature	Low	July 13	9	1.87	0.19	0.69	0.06	0.78	0.06	G7K8P
Mature	Medium	June 19	9	2.57	0.27	0.77	0.04	0.84	0.06	F7J1P
Mature	Medium	June 19	9	1.99	0.28	0.70	0.09	0.74	0.11	G1K9P
Mature	High	June 19	9	3.03	0.27	0.82	0.02	0.89	0.05	F7J0P
				NSA Mixed						
Mature	Low	July 31	9	1.91	0.27	0.75	0.03	0.83	0.04	Q1V2M
Mature	High	July 4	9	3.09	0.33	0.82	0.03	0.89	0.07	T0P5M
				SSA Mixed						
Disturbed	Medium	July 26,	9	2.42	0.33	0.80	0.04	0.84	0.04	H2D1M
Intermediate	Medium	June 25		3.01	0.35	0.86	0.03	0.91	0.03	D9I1M
Mature	Medium	Aug. 14	8	1.23	0.19	0.58	0.05	0.55	0.06	H3D1M
Mature	High	July 15	9	2.96	0.35	0.82	0.03	0.90	0.05	G4I3M

Productivity is the net primary productivity assessed from the tree trunk diameter and age, n is the number of photographs analyzed, s.d. is standard deviation, FIPAR diffuse is the fraction of diffuse photosynthetically active radiation intercepted by the canopy, and FIPAR direct is the similar fraction for direct radiation. Both FIPAR values are determined by the canopy gap fraction and are therefore closely related to L_e, indicating the importance of L_e as a stand parameter. Site codes are defined in the text.

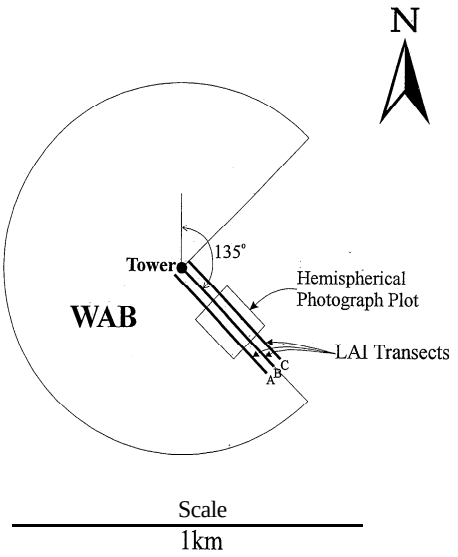

Figure 1. Locations of LAI transects and the heimispherical photograph plot in the wind-aligned blob (WAB) at the tower sites. In SOA, the LAI transects runs from the tower in the southwest direction. In SYJP and NYJP, the transects runs in both southeast and northwest directions from the tower.

the program LAICALC. Calculating formulae and operation of LAICALC are described in detail in the LAICALC manual *[Rich et al.,* 1995] following the method of *Chen et al.* [1991]. In order to compare hemispherical photography technique and LAI-2000 results, the gap fractions from the photographs were similarly separated into five zenith angles from 0 to 75°.

3.5. Tree Destructive Sampling Procedures

A complete description of field and laboratory methods and model development of the allometric equations is provided by *Gower et al.* [this issue]. Therefore, for brevity, we will summarize the methods used to directlv estimate leaf and stem area. In each stand, four to five plots were established and species, crown class, and diameter were determined for ail trees with a diameter at breast height (1.3 m) $D_{bh} > 2.5$ cm. Gower et al. selected trees of varying diameter to represent the range of tree sizes measured in the plots. In August 1994, two dominant, three codominant, three intermediate, and two suppressed trees were destructively sampled from each intensive site. All trees were harvested from late July to early August, well before leaf fall.

Trees were cut at the soil surface, and total tree height and length of the live crown were measured. Stem area was calcu-Iated by assuming that the stem section from the soil to D_{bh}, from D_{bh} to base of live crown, and from base of live crown to the stem top approximated a frustrum of a neiloid, a frustrum of a paraboloid and a cone, respectively *[Gower et al.,* this issue]. The live crown was marked into thirds (top, middle, and lower), and all live and dead branches from each position were cut and weighed separately. One branch from each canopy position was randomly selected for detailed analysis in the field immediately after each tree was felled. *Populus tremuloides* branch samples were divided into foliated twig and nonfoliage-bearing branches. *Pinus banksiana* branches were divided into current, 1-, 2-, and >3-year-old shoots (needles + twig) and nonfoliage-bearing branches. *Picea mariana* and *P. glauca* branches were divided into current, l-2, 3-4, and >5-year-old shocts and nonfoliage-bearing branches. Foliage-bearing twigs were mixed thoroughly, and approximately 30-50 shoots were selected for each shoot age class and canopy position combination. The fresh mass of each component was determined using an electronic balance, and the sample was placed in a labeled bag and stored in a cold room until transported to Wisconsin. Approximately 5-10 shoots were used for specific leaf area measurement. The volume displacement method described in the appendix was used for measuring the hemi-surface area of needles.

Regression models of the form log,, Y = a + b log,, X were used to correlate stem and foliage area to $D_{,,}$. A $\log_{10}$ – log,, transformation was needed to correct for nonhomogeneous variance of the independent variable. Stem area was highly correlated to stem diameter, and the r^2 values ranged from 0.92 to 0.99 *[Gower et al.,* this issue]. Total leaf area per tree was highly correlated to stem diameter for most stands; the r^2 values ranged from 0.75 to 0.98, with the majority exceeding 0.85 *[Gower et al.,* this issue].

To obtain the woody-to-total area ratio (α) for mature stands, three or four trees were harvested in SOBS, SOJP, and NOJP for the direct measurements of the total surface areas of needles and woody materials. The individual tree measurements were extrapolated to the whole stand using D_{bh} measurements. The α values were found to be 0.16, 0.32, and 0.28 for SOBS, SOJP, and NOJP, respectively *[Chen,* 1996a].

3.6. Shoot Samples and Analysis

From each intensive conifer site, shoot samples were taken in each summer IFC in 1994 to obtain the within-shoot clumping factor. Trees of a stand were first grouped into three classes: dominant, codominant, and suppressed, and each tree was divided into three height classes: top,. middle, and bottom, creating nine shoot classes per stand. Three to 10 shoots per class were taken for a total of 27-90 shoots per stand, for laboratory analysis. A video camera and computer system (AgVision, Decagon Devices, Inc., Pullman, Washington) was used to determine the projected area of the shoots, and a volume displacement method was used to measure the needle area (see appendix). The total needle area in a shoot and the total imaginary shoot area obtained from the projected shoot area were used to calculate the needle-to-shoot area ratio *[Chen,* 1996a].

4. Results and Discussion

4.1. Comparison of the Effective LAI

Figure 2 illustrates the spatial distribution of L_e along the transects during the IFC in 1993 at six intensive sites. Similar measurements were made in each IFC in 1994 to obtain the seasonal variation of L_e for each stand. Except for SOJP, LAI varied substantially, especially in the mature conifer stands. The standard deviation (error) in L_e is 0.66 (0.069) for SOBS, 0.22 (0.028) for SOJP, 0.44 (0.046) for SYJP, 0.15 (0.016) for SOA, 0.50 (0.052) for NOBS, 0.28 (0.032) for NOJP, 0.26 (0.026) for NYJP, and 0.15 (0.045) for NOA. SOJP transects were established in a very uniform part of the stand without tall understory species. In NOJP there are many sharp spikes in L_e distribution because of the presence of shrub green alder (AZ-*nus crispa*) which appears in large clumps up to 5 m in diameter and 3-4 m in height [*Vogel,* 1997]. Both black spruce stands (SOBS and NOBS) have pronounced variations at 50-100 m

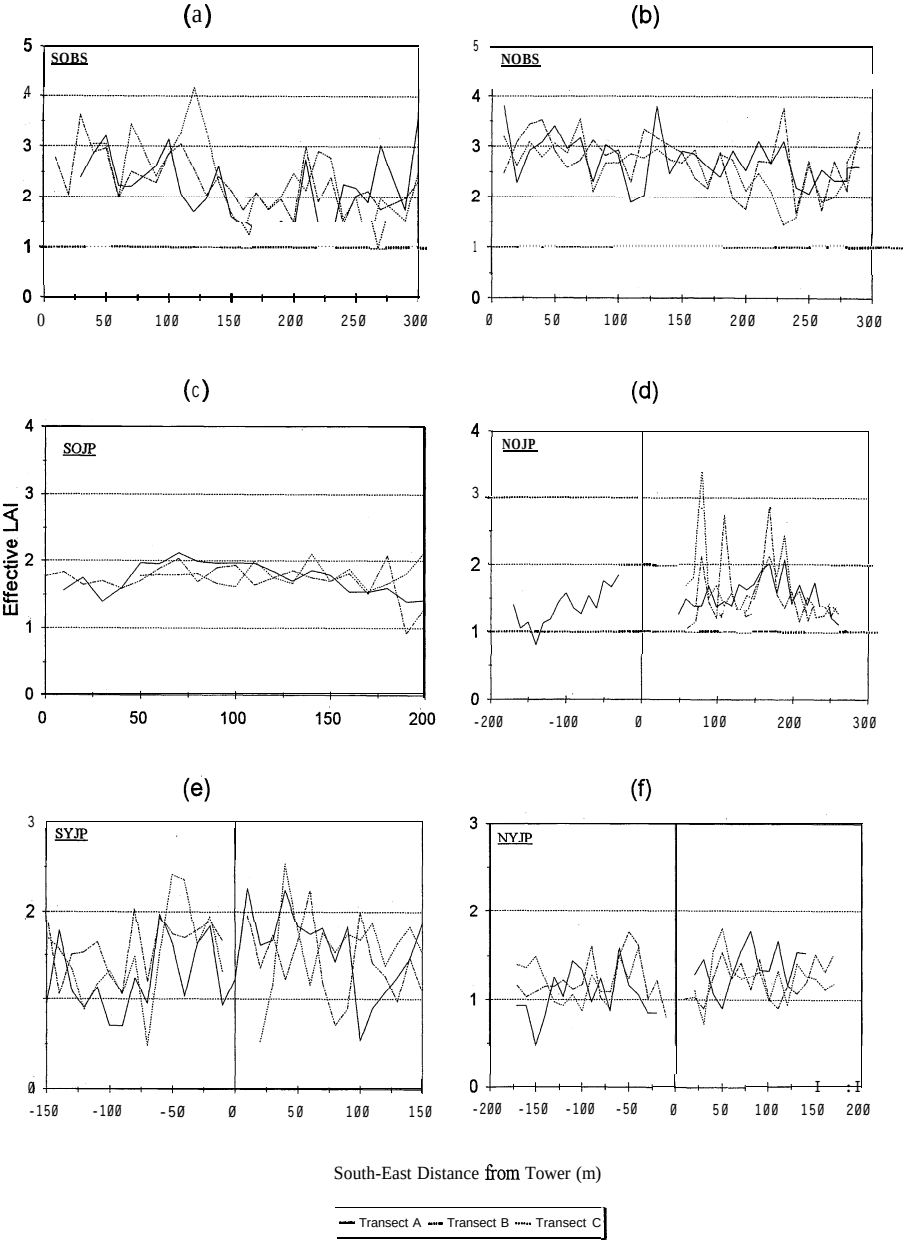

Figure 2. Measurements of effective LAI along the LAI transects in six conifer tower sites where a positive (negative) value on the abscissa indicates the southeast (northwest) distance from the tower.

scales which may be due to small topographic variations affecting the drainage pattern and tree growth. Although all these stands were selected for homogeneous species composition and stand structure, these data clearly indicate the difficulty in obtaining a stand average of LAI and the importance of the location of measurements.

Point estimates of L_e obtained using hemispherical photography and LAI-2000 were in good agreement (Figure 3). Because of the relative uniformity of the SOJP site, the measurements compare particularly well. However, in the SOBS, larger spatial inhomogeneities exist, and measurement locations of these two instruments were not always identical. Therefore much of the discrepancy may be due to slight differences in sample location. On the stand average, such location difference is much reduced.

Stand averages of L_e obtained from the LAI-2000 and hemispherical photograph techniques were highly correlated with r^2 = 0.8 1 (Figure 4), and the slope of the regression line was not significantly different from 1 $(p < 0.01)$, indicating the usefulness of these techniques for measuring the gap fraction at various zenith angles. We caution, however, that both techniques can suffer from the same problem: scattering of light within the canopy, and in Figures 2 and 3, no corrections were made to the L_e values for the multiple scattering effect for the purpose of direct comparison. In order to minimize this effect, LA-I-2000 uses only the blue light (400-490 nm) and assumes all diffuse blue light originates directly from the sky (i.e., leaves in the blue band are totally black). Although blue reflectance of leaves is the smallest in the solar spectrum, it is still significantly larger than zero (about 3-6%). In open canopies the

Table Al. Equations for Converting Measurements of Needle volume V, Average Length l, and Number n to Hemi-surface Area for Several Different Shapes of Needle Cross Section

Shape	Equation	Example
Cylinder	$\sqrt{\pi} \times \sqrt{(Vnl)}$	$1.77\sqrt{(Vnl)}$
Square	$2\sqrt{(Vnl)}$	$2.00\sqrt{(Vnl)}$
Diamond	$2\sqrt{[(1+x^2)/2x]}\sqrt{(Vnl)}$	x = (major axis)/(minor axis)
	$x = 1$	$2.00\sqrt{(Vnl)}$
	$x = 2$	$2.24\sqrt{(Vnl)}$
	$x = 3$	$2.58\sqrt{(Vnl)}$
Ellipse	$0.5\sqrt{(\pi x)}$ x $(1 + 1/x)$ x $\sqrt{(Vnl)}$	x = (major axis)/(minor axis)
	$x = 1$	$1.77\sqrt{(Vnl)}$
	$x = 2$	$1.88\sqrt{(Vnl)}$
	$x = 3$	$2.05\sqrt{(Vnl)}$
Rectangle	$\sqrt{x}$ x $(1 + 1/x)$ x $\sqrt{(Vnl)}$	x = length/width
	$x = 1$	$2.00\sqrt{(Vnl)}$
	$x = 2$	$2.12\sqrt{(Vnl)}$
	$x = 3$	$2.31\sqrt{(Vnl)}$
Cylinder sections	$[\sqrt{(x/\pi)} + \sqrt{(\pi/x)}] \times \sqrt{(Vnl)}$	x = number of sections ≥ 2
	$x = 2$	$2.05\sqrt{(Vnl)}$
	$x = 3$	$2.00\sqrt{(Vnl)}$
	$x = 5$	$2.05\sqrt{(Vnl)}$

mature jack pine. Therefore a crude conversion factor from L_e to LAI is 1.8 for mature black spruce (assuming $\gamma_E = 1.4$ and $(1 - \alpha) = 0.84$) and 1.3 for mature jack pine (assuming $\gamma_E = 1.45$ and $(1 - a) = 0.68$). According to our measurements, LAI of boreal jack pine and aspen species have similar values, falling in the range 1-4, but the prevailing black spruce has a larger range, 1-6. All boreal species are highly clumped. Stands with large LAI values are still quite open, as evidenced in the small effective LAI values, because of foliage clumping at tree, branch, and shoot levels.

Appendix: Volume Displacement Method

The surface area for conifer shoots can be measured by several methods, but the two most common are volume displacement and projected area of detached needles using an optical planimeter. Because needle surface area is the measurement desired, projected-area measurements with optical planimeters are insufficient unless the appropriate shape factors are included to calculate the hemi-surface area (HSA) of needles.

Using the optical planimeter is tedious because needles have to be carefully aligned so as to present their maximum area to the planimeter. Since many conifer needles are curved or twisted by variable amounts, projected area measurements are subject to considerable error unless great care is taken. Given the measured needle projected area of all the needles that have been detached from the shoot and a known cross-sectional shape for the needles, the surface area can be calculated and divided by 2 to get the HSA.

A faster method that is more reliable than the planimeter method and does not require an expensive optical planimeter is the volume displacement method. This method requires a reasonably good, top-loading electronic balance, something common to any lab. The method we use is similar to that reported by *Beets* [1977]. A shoot is detached from a tree and submersed in a container of water (with 5% detergent added) that is placed on a top-loading electronic balance. The volume of the needles plus twig is equal to the weight of water displaced by the shoot. The needles then are removed from the twig and counted, and their average length is measured. The volume of the twig then is measured in the'same manner as the shoot, so that the needle volume is the difference between the shoot and twig volumes. Knowing the shape of the cross-sectional area of a needle permits estimation of the needle surface area. Shapes of needle cross sections can vary, especially between sun and shade leaves *[Brand,* 1987]. However, such variations in shape usually do not appear to cause serious errors. More precise schemes for accommodating systematic patterns of needle cross-sectional shape are possible with regression approaches [Johnson, 1984], but this was not necessary with black spruce and jack pine.

The measurements of needle volume, length, and number can be converted to needle surface area using simple geometry. The equations for several different needle shapes are given in Table Al.

An additional measurement that is valuable in converting shoot measurements to correction factors for indirect LAI measurements is the length of the intact shoot and the diameter of the intact shoot. These dimensions are of an effective cylinder that would just match (in an average sense) the outside envelope of the intact shoot (Table A2).

Careful measurements of total surface area were done on

Table A2. Equations Suggested for Calculating the Total Needle Area (Sn) Using the Volume-Displacement Technique for Several Shapes

Shape	Sn	Species
Square	$4.00\sqrt{(Vnl)}$	blue spruce
Ellipse (1:3 ratio of axes)	$4.35\sqrt{(Vnl)}$	Douglas fir
Cylinder	$3.54\sqrt{(Vnl)}$	
Hemi-cylinder	$4.10\sqrt{(Vnl)}$	black pine
Rectangle		
Width = (length/lo)	$6.96\sqrt{(Vnl)}$	
Width = (length/4)	$5.00\sqrt{(Vnl)}$	
Width = (length/3)	$4.87\sqrt{(Vnl)}$	
Width = (length/2)	$4.24\sqrt{(Vnl)}$	
Diamond (1:1.5 ratio of two axes)	$4.16\sqrt{(Vnl)}$	black spruce

V is the volume displacement by the needles, n is the number of needles, and l is the average length of the needles. The woody twig volume can be used to get the twig contribution to surface area using $n = 1$ and the length of the twig.

Table A3. Comparison of Needle Area Measured by the Volume Displacement Method and the Optical Planimeter Method

	Needle Area, mm^2	
Species	Optical Planimeter	Volume Displacement
Blue spruce	3276	3216
Douglas fir	9990	9705
Black pine	4084	3900

several species by both the volume displacement method and optical planimeter method (Table A3).

With Douglas fir, if detergent was not added to the water, the volume displacement method overestimated the surface area by 35% in one case and 39% in a second case because of entrapped air. The cross-sectional area of blue spruce was a square, of Douglas fir an ellipse with a ratio of major to minor axes of 3:1, and black pine a half-cylinder.

Acknowledgments. We jointly acknowledge the coordinating effort made by the BOREAS operating offices during the field experiment in Saskatchewan and Manitoba. Jason Vogel of the University of Wisconsin contributed to the destructive measurements. J. Chen thanks Martin Guilbeault, Darcy Delgatty, Onmanda Niebergall, Debbie Miller, and Jason Nelson for their contributions to field and laboratory measurements. P. Rich thanks Yvette Alger, Venessa Peterson, Richard Fournier, and Jason Vogel for assistance with collecting the hemispherical photographs. S. Plummer thanks Neil Lucas for help in the collection of the Sunfleck ceptometer and LAI-2000 data and NERC for funding the field work. This work was supported by the Canada Centre for Remote Sensing, the Kansas Applied Remote Sensing Program, the Kansas Biological Survey, the Kansas Center for Computer Aided Systems Engineering, NASA grant NAG5-2358, and the University of Kansas Research Development and General Research Funds.

References

Anderson, M. C., Studies of the woodland light climate, I, The photographic computation of light condition, *J. Ecol.*, *52, 27-41,* 1964.

Beets, P., Determination of the fascicle surface area for *Pinus radiata, N. Z. J. For. Sci., 7, 397-407, 1977.*

Bonan, G. B., Importance of leaf area index and forest type when estimating photosynthesis in boreal forests, *Remote Sens. Environ.*, 43, 303-314, 1993.

Bonhomme, R., C. Varlet Granger, and P. Chartier, The use of hemispherical photographs for determining the leaf area index of young crops, *Photosynthetica*, *8,* 299-301, 1974.

Brand, D. G., Estimating the surface area of spruce and pine foliage from displaced volume and length, *Can. J. For. Res., 17,* 1305-1308, 1987.

Chen, J. M., Optically based methods for measuring seasonal variation in leaf area index in boreal conifer stands, *Agric. For. Meteorol., 80,* 135-163, 1996a.

Chen, J. M., Canopy architecture and remote sensing of the fraction of photosynthetically active radiation absorbed by boreal conifer forests, *IEEE Trans. Geosci. Remote Sens.*, *34, 1353-1368,* 1996b.

Chen, J. M., and T. A. Black, Defining leaf area index for non-flat leaves, *Plant Cell Environ., 15, 421-429,* 1992a.

Chen, J. M., and T. A. Black, Foliage area and architecture of plant canopies from sunfleck size distributions, *Agric. For. Meteorol., 60,* 249-266, 1992b.

Chen, J. M., and J. Cihlar, Plant canopy gap size analysis theory for improving optical measurements of leaf area index, *Appl. Opt., 34,* 6211-6222, 1995a.

Chen, J. M., and J. Cihlar, Quantifying the effect of canopy architecture on optical measurements of leaf area index using two gap size analysis methods, *IEEE Trans. Geosci. Remote Sens.*, *33, 777-787,* 1995b.

Chen, J. M., and J. Cihlar, Retrieving leaf area index of boreal conifer forests using Landsat TM images, *Remote Sens. Environ., 55,* 153–162, 1996.

Chen, J. M., T. A. Black, and R. S. Adams, Evaluation of hemispherical photography for determining plant area index and geometry of a forest stand, *Agric. For. Meteorol., 56,* 129-143, 1991.

Chen, J. M., P. D. Blanken, T. A. Black, M. Guilbeault, and S. Chen, Radiation regime and canopy architecture in a boreal aspen forest, *Agric. For. Meteorol., 86,* 107-125, 1997.

Clark, D. B., D. A. Clark, P. M. Rich, S. B. Weiss, and S. F. Oberbauer, Landscape-scale evaluation of understory light and canopy structure: Methods and application in a neotropical lowland rain forest, *Can. J. For. Res., 26, 747-757, 1996.*

Evans, G. C., and D. E. Coombe, Hemispherical and woodland canopy photography and the light climate, *J. Ecol.*, 47, 103-113, 1959,

Fassnacht, K., S. T. Gower, J. M. Norman, and R. E. McMurtrie, A comparison of optical and direct methods for estimating foliage surface area index in forests, *Agric. For. Meteorol., 71,* 183–207, 1994.

Galo, A. T., P. M. Rich, and J. J. Ewel, Effects of forest edges on the solar radiation regime in a series of reconstructed tropical ecosysterns, *Am. Soc. Photogramm. Remote Sens. Tech. Pap.,* 98–108, 1992.

Gower, S. T., and J. M. Norman, Rapid estimation of leaf area index in forests using the LI COR LAI 2000, *Ecology, 72,* 1896–1900, 1990.

Gower, S. T., J. G. Vogel, T. K. Stow, J. M. Norman, S. J. Steele, and C. J. Kucharik, Carbon distribution and aboveground net primary production in aspen, jack pine, and black spruce stands in Saskatchewan and Manitoba Canada, *J. Geophys. Res.,* this issue;

Grier, C. C., K. M. Lee, and R. M. Archibald, Effects of urea fertilization on allometric relations in young Douglas fir trees, *Can. J. For. Res., 15, 900-904,* 1984.

Johnson, J. D., A rapid technique for estimating total surface area of pine needles, *For. Sci., 30,* 913-921, 1984.

Kucharik, C. J., J. M. Norman, L. M. Murdock, and S. T. Gower, Characterizing canopy nonrandomness with a multiband vegetation imager (MVI), J. *Geophys. Res.,* this issue.

Lang, A. R. G., Application of some of Cauchy's theorems to estimation of surface areas of leaves, needles and branches of plants, and light transmittance, *Agric. For. Meteorol.,* 55, 191-212, 1991.

Lang, A. R. G., and Y. Xiang, Estimation of leaf area index from transmission of direct sunlight in discontinuous canopies, *Agric For. Meteorol., 35, 229 -243, 1986.*

Lerdau, M. T., N. M. Holbrook, H. A. Mooney, P. M. Rich, and J. L. Whitbeck, Seasonal patterns of acid fluctuations and resource storage in the arborescent cactus *Opuntia excelsa* in relation to light availability and size, *Oecologia,* 92, 166-171, 1992.

Leverenz, J. W., and T. M. Hinckley, Shoot structure, leaf area index and productivity of evergreen conifer stands, *Tree Physiol., 6,* 135-149, 1990.

Lin, T., P. M. Rich, D. A. Heisler, and F. J. Barnes, Influences of canopy geometry on near-ground solar radiation and water balances of pinyon-juniper and ponderosa pine woodlands. *Am. Soc. Photogramm. Remote Sens. Tech. Pap., 285-294, 1992.*

Miller, J. B., A formula for average foliage density, *Aust. J. Bot., 15,* 141-144, 1967.

Miller, E. E., and J. M. Norman, A sunfleck theory for plant canopies, I, Lengths of sunlit segments along a transect, *Agron. J., 63,* 735–738, *1971.*

Mitchell, P. L., and T. C. Whitmore, Use of hemispherical photographs in forest ecology: Calculation of absolute amount of radiation beneath the canopy, Oxford For. Inst., Oxford, England, 1993.

Neumann, H. H., G. den Hartog, and R. H. Shaw, Leaf area measurements based on hemispheric photographs and leaf-litter collection in a deciduous forest during autumn leaf-fall, *Agric. For. Meteorol., 45,* 325-345, 1989.

Nilson, T., A theoretical analysis 'of the frequency of gaps in plant stands, *Agric. Meteorol., 8, 25-38,* 1971.

Norman, J. M., Crop canopy photosynthesis and conductance from leaf measurements, workshop prepared for LI-COR, Inc., Lincoln, Nebr., 1988. (From Welles, J. M., Some indirect methods of estimating canopy structure, in *Instrumentation for Studying Vegetation Canopies for Remote Sensing in Optical and Thermal Infrared Region, edited by N. S. Goel and J. M. Norman, Remote Sens. Rev., 5*(1), 31-43, 1988.)

Norman, J. M., and G. S. Campbell, Canopy structure, in *Plant Phys-*

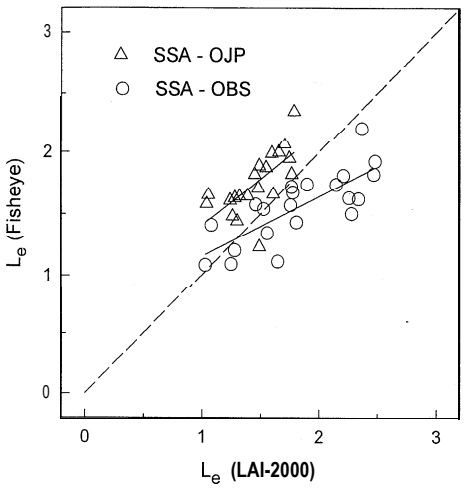

Figure 3. Comparison of individual effective LAI (L_e) measurements in two stands by hemispherical photography and the LI-COR LAI-2000.

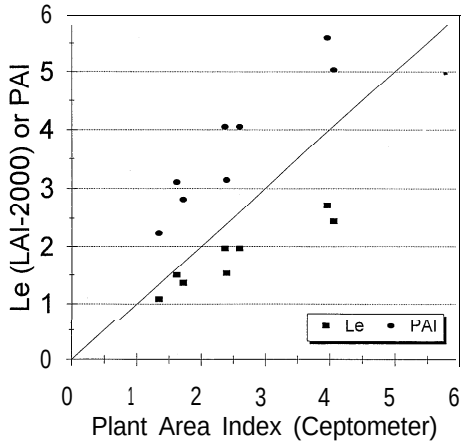

Figure 5. Comparison of plant area index (PAI) measured using the Sunfleck Ceptometer with L_e measurements by LI-COR LAI-2000 and with PA1 obtained from L_e and foliage clumping indices.

contribution of scattered blue light is small compared with that from the sky; therefore the problem is less serious. The same principle applies to the gap fraction measurement at the various zenith angles. At large zenith angles, the canopy gap fraction is always small, even in open stands, and therefore the scattering problem is more serious. In the calculation of L_e, the gap fractions at large zenith angles are more important than those at small zenith angles because of the sin θ weight (1), suggesting that the scattering effect should not be overlooked. In photographs the scattering effect also exists but in a different way. Leaves at the top of a canopy under bright light appear to be much brighter than the foliage under them. These bright leaves are more easily seen at small zenith angles than at large zenith angles, and therefore the absolute distortion of the gap fraction is larger at smaller zenith angles when a fixed threshold value is used to distinguish leaves from the sky. The relative change in the gap fraction due to the distortion is complicated by the angular resolution of the hemispheric image. In a coarse image, many small gaps at large zenith angles may be missed in the digitization, which may even overcompensate the scattering effect, resulting in underestimation of the gap fraction. Because of the different limitations of these techniques, *Chen et al.* [1991] found that foliage angle distributions derived from gap fractions measured using these techniques were considerably different. In this study, problems with uneven illumination on foliage were minimized by acquiring photographs only in cases of very even backlighting (typically, predawn), and the photographs were digitized to images of size 512 x 480 to achieve a reasonable angular resolution and reduce the loss of small gaps near the horizontal direction. Compared with LAI-2000, hemispherical photographs have the advantage of recording permanent images of the canopy which can be used to investigate the scattering effect. A summary of L_e measurements in BOREAS auxiliary sites is given in Table 2 according to species and estimated classes of net primary productivity.

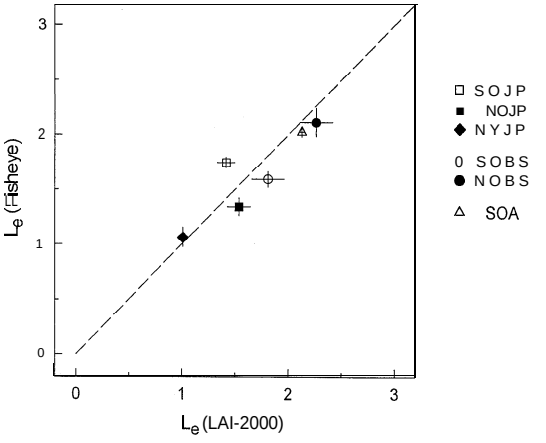

Figure 4. Comparison of the mean L_e values for the seven tower sites obtained from hemispherical photography and the LI-COR LAI-2000.

Figure 5 shows the comparison between measurements from the LAI-2000 and the Sunfleck Ceptometer for eight jack pine sites within the SSA, six from IFC-2 and two from IFC-93 (SOJP and SYJP). The measurements of the Ceptometer are regarded as the PAI because the below-canopy PAR measurements are affected by all aboveground materials including leaves, branches, and tree trunks. The direct LAI-2000 measurements are taken as L_e, and the PA1 on the ordinate is based on measurements of LAI-2000 and TRAC assisted with laboratory analysis on shoot samples. It is calculated as L_e x 1.46/0. 7 1, where 1.46 is the needle-to-shoot area ratio and 0.71 is the element clumping index (see Table 3). Both the L_e and PA1 estimates are highly correlated to the Ceptometer measurements, but the slopes of the regression lines are significantly different from 1. The Ceptometer PA1 results are larger than L_e but smaller than PA1 obtained from the combination of LAI-2000 and TRAC measurements. By taking the finite-length averaging method, the Ceptometer measurements removed the effect of foliage clumping at scales larger than the averaging length (0.8 m), making its measurements larger than L_e obtained from LAI-2000, which include the effect of foliage clumping at all scales. However, in the Ceptometer measurements the effect of foliage clumping at scales smaller than the averaging length remains. The bulk of the effect is due to clumping within shoots, which is a factor of 1.46 in jack pine

Table 3. Summary of Optical and Allometric LAI Measurements

Period	L_e	γ_E	Ω_E	$(1-\alpha)$	Optical LAI	Allometic LAI
			SOBS			
IFC-93	2.27	(1.42)	(0.70)	(0.84)	3.87	
IFC-1, 94	2.35	1.30	0.70	(0.84)	3.67	
IFC-2, 94	2.45	1.36	0.70	(0.84)	4.00	6.3
IFC-3, 94	2.27	1.42	0.70	0.84	3.87	
			SOJP			
IFC-93	1.75	(1.51)	(0.71)	(0.68)	2.53	
IFC-1, 94	1.77	1.28	0.71	(0.68)	2.17	
IFC-2, 94	1.87	1.46	0.71	(0.68)	2.61	2.5
IFC-3, 94	1.76	1.51	0.71	0.68	2.54	
			SYJP			
IFC-93	1.46	(1.37)	(0.72)	(0.95)	2.64	
IFC-1, 94	1.51	1.43	0.72	(0.95)	2.85	
IFC-2, 94	1.55	1.52	0.72	(0.95)	3.10	2.8
IFC-3, 94	1.57	1.37	0.72	(0.95)	2.83	
			SOA			
IFC-93						
IFC-1, 94	2.02	1	0.82	0.70	1.72	
IFC-2, 94	2.42	1	0.70	0.75	2.59	3.3
IFC-3, 94	2.20	1	0.76	0.73	2.11	
			NOBS			
IFC-93	2.70	(1.50)	(0.71)	(0.84)	4.79	
IFC-1, 94	2.66	1.32	0.71	(0.84)	4.15	
IFC-2, 94	2.75	1.40	0.71	(0.84)	4.55	5.0
IFC-3, 94	2.71	1.50	0.71	0.84	4.81	
			NOJP			
IFC-93	1.55	(1.42)	(0.82)	(0.72)	1.93	
IFC-1, 94	1.61	1.15	0.82 .	0.72	1.63	
IFC-2, 94	1.64	1.30	0.82	0.72	1.87	2.2
IFC-3, 94	1.64	1.42	0.82	0.72	2.04	
			NYJP			
IFC-93	1.21	(1.45)	(0.95)	(0.97)	1.79	
IFC-1, 94	1.25	1.22	0.95	(0.97)	1.56	
IFC-2, 94	1.25	1.27	0.95	(0.97)	1.62	2.0
IFC-3, 94	1.27	1.45	0.95	(0.97)	1.88	
			NOA			
IFC-93						
IFC-1, 94	2.25	1	0.79	0.80	2.27	
IFC-2, 94	2.25	1	0.72	0.80	2.50	3.6
IFC-3, 94	2.09	1	0.88	0.78	1.85	

Values in parentheses are estimated. Stand abbreviations and periods of the intensive field campaigns (IFCs) are defined in the text.

stands. This factor makes PA1 based on LAI-2000 and TRAC much larger than the PA1 from the Ceptometer. We conclude from this comparison that *Lang and Xiang*'s [1986] finite-length averaging technique is effective in removing the effect of foliage clumping at large scales but underestimates PA1 or LAI because of foliage clumping at small scales, especially clumping within shoots.

4.2. Comparison of LAI Measurements

Measurements of L_e are an important step in optical measurements of LAI, but to obtain LAI, other parameters in (5) need to be quantified. They include the woody-to-total area ratio (α), the element clumping index (Ω_E), and the needle-to-shoot area ratio (γ_E). The full details of the methods for obtaining these parameters are given by *Chen* [1996a] and *Gower et al.* [this issue]. Table 3 summarizes the average values of each component leading to the LAI estimates based on optical measurements. The numbers in parentheses are estimated values based on measurements made in other periods. The γ_E values in IFC-93, for example, are taken as the same as those in IFC-3, 94. *Chen* [1996a] found that Ω_E for conifer does not vary significantly throughout the summer season (from IFC-1 to IFC-3) but is weakly dependent on the solar zenith angle. Therefore only one value of Ω_E was suggested for a conifer stand after using a weighting scheme for individual Ω_E values at different solar zenith angles. Ω_E does not vary with season because the foliage clumping effect is the result of large gaps between tree crowns and branches which do not change seasonally. Also according to *Chen* [1996b], L_e from LAI-2000 were 0–25% (with an average of 15.3%) smaller than those from TRAC for six conifer stands. Similarly, *Chen et al.* [1997] reported that LAI-2000 underestimates L_e by 15% in an aspen stand (SOA) when compared with radiation tram measurements. The underestimation of L_e is attributed to the blue light scattering effect on LAI-2000 measurements. Both TRAC and the radiation tram are able to separate the direct

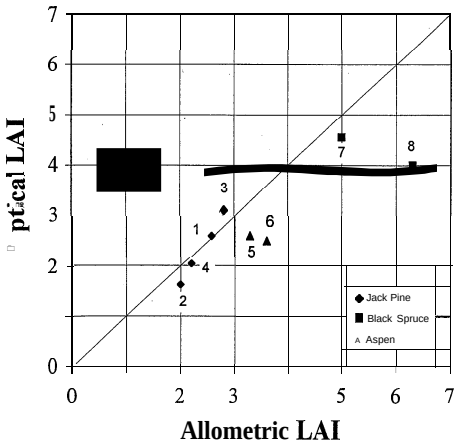

Figure 6. Comparison of optical LAI with allometric LAI for seven tower sites and an auxiliary site (NOA).

and diffuse radiation components and remove most of the scattering effect. Therefore the stand averages of L_e presented in Table 3 were increased by 15% from the direct readings of LAI-2000 shown in Figures 3 and 4 (this correction is made in Figure 2).

Except for SOBS, labeled 8 in Figure 6, there was good agreement between direct and indirect estimates of LAI. The discrepancy in SOBS is likely because of the large spatial variability and difference in location between the direct and indirect measurements. The analysis of the results can benefit from comparison with the results from NOBS. Both these two black spruce stands are spatially highly variable, as evident in the L_e trace (Figure 2). The eastern section of NOBS containing the LAI transects is located in the dense part of the stand and has LAI values larger than the average surrounding conditions. The LAI transects in SOBS ran through an open part of the canopy, which brings down the average L_e values and therefore the LAI values in the optical results. Although LAI-2000 suffers from its own problems (namely, the scattering effect), the instrument has shown good repeatability in the same stands (Table 3). Relatively speaking, the LAI transects in NOBS have larger L_e values than those in SOBS. The values of γ_E and Ω_E in Table 3 differ only slightly between these two stands, showing their similarity. From the consistency of these optical results, we therefore expect larger LAI values in NOBS than in SOBS over the transects. While the optical and allometric LAI values agree very well in NOBS, they differ by 45% in SOBS. The difference in SOBS may have resulted from the different locations of the allometric plots and LAI transects. There were four 25 m × 25 m plots located about 60, 85, 110, and 135 m east of the flux tower. Their LAI values are 9.10, 6.34, 5.02, and 4.86, respectively. These plots were mostly the average-to-dense part of the stand, while the LAI transect consists of essentially a dense (O-150 m) and an open section (150-300 m). The difference in the L_e values in the two sections is about 27%. This difference would have caused the mean L_e (as well as LAI) over the whole transect to be 13.5% smaller than that over the first part of the transects. The optical LAI of the dense section is 4.5. The allometric LAI plots were located near this section. It would be therefore more meaningful to compare the mean allometric LAI with the optical LAI obtained from the first 150 m of the transects. The difference between 6.3 and 4.5 is 33%, which is within the sum of measurement errors of both techniques. To further determine the cause for the difference, we applied the allometric equation $\log_{,,}(Y) = -0.645 + 1.806 \times \log_{,,}(X)$ [*Gower et al.,* this issue] to D_{bh} values measured in a 10 m × 20 m area located in the middle of the first part of the LAI transects and obtained an LAI value of 3.6. This transect value is considerably smaller than the average allometric plot value, indicating large spatial inhomogeneity. The large spatial variation raised questions concerning the mean LAI value for the stand. To address this issue, in 1996 we acquired additional LAI-2000 measurements 500 m west of the tower and obtained a mean L_e value of 2.3. Using the γ_E, Ω_E, and α values for IFC-2 in Table 3, this L_e value is converted to LAI = 3.8. According to our analysis (see the next section) and comparison with the allometric results, TRAC underestimates the extreme clumping effect in black spruce stands, resulting in a negative bias in LAI values by about 10%. We therefore recommend 4.2 ± 1.0 as the LAI representing the footprint area of the eddy covariance tower in SOBS.

The optical LAI values from the remaining six stands (SOJP, SYJP, NOJP, NYJP, SOA, and NOA) compare reasonably well with the allometric values. These stands are generally more homogeneous at large scales than SOJP and NOJP, causing smaller problems in the LAI comparison. The remaining largest differences between optical and allometric LAI results are 36% for NOA and 34% for SOA. Although these differences are within the sum of experimental errors of both techniques, they may also be partly due to the spatial variability. *Chen et al.* [1996] found that the variation of LAI across a 300 m transect in SOA is about 20%. In both stands, optical results are smaller than allometric results. It is likely that the gap size analysis technique underestimates the clumping effect due to the difficulty in removing the penumbra effect in the tall stands. It is also possible that the 15% correction for the blue light scattering effect on L_e measurements is too small for the stands with large leaf reflectance and transmittance.

4.3. Limitation of Optical Techniques in Highly Clumped Black Spruce Stands

After consideration of the spatial variability in SOBS, the optical LAI is still smaller than the allometric value. Although the LAI measurements suffer from considerable errors, the difference may also result from a limitation in the optical techniques. Tree crowns of black spruce are typically long and narrow, with 40–50% of foliage concentrated in the top conical part of the tree crown. Figure 7 shows destructive measurements made in SOBS. The distribution of foliage area with height indicates that a large proportion of foliage is located near the bottom of the conical part of the tree crown, making the core of the cone impermeable to the solar beam. This pattern of foliage distribution may be an extreme case and is highly clumped. Although the TRAC is able to quantify the effect of foliage clumping on LAI measurements, it assumes that all foliage clumps larger than the shoot are penetrable by light. This assumption is necessary in the calculation of the clumping index because if no gaps are observed within a clump, it becomes impossible to estimate the foliage area inside it. The dense top of black spruce crowns allows very little light penetration and hence violates this assumption. Under such extreme conditions, the TRAC underestimates the clumping effect and LAI.

According to the foliage density distribution presented in Figure 7, it is possible to estimate this unconventional clumping effect. Assuming 50% foliage is grouped in the conical part

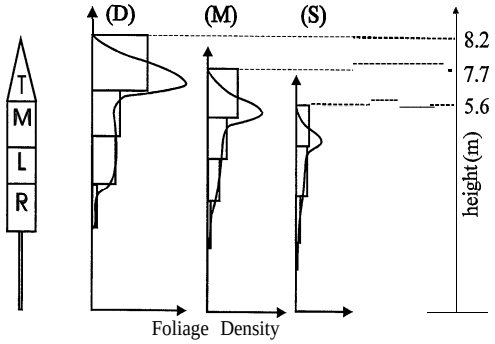

Figure 7. Profiles of foliage area of three trees classified as dominant (D), codominant (M), and suppressed (S) in a mature black spruce stand in the southern study area. In destructive sampling, each tree crown was separated into four sections: top (T), middle (M), low (L), and residual (R). The area of the rectangles indicates the average foliage area for the height class, and the curves are reconstructed from the average values, assuming the conical + cylindrical crown shape. The measurements are drawn to scale.

of the crown and the shadow areas of the crown sections T, M, and L are approximately the same on the ground (the projection of section R can be ignored), the extreme clumping at the tree top then reduces the projection on the ground by 25%. This means the canopy gap fraction would decrease by 25% if no such extreme clumping occurs at the tree top. With the canopy gap fraction of about 0.3 at the zenith angle of 40" in SOBS, the reduction of the canopy gap fraction by 25% would cause L_e to increase by 20%. However, the increase of small canopy gaps by 25% would increase the Ω_E, calculated from the canopy gap size distribution, by 10%, resulting in a 10% decrease in LAI. The net effect of such extreme clumping is then to increase LAI by about 10%. We therefore believe the optical methods underestimate LAI by about 10% in black spruce stands. If this correction is made, the optical LAI is 5.3 for NOBS and 4.4 for SOBS over the whole SE transect or 5.2 over the first 150 m of the SE transect and 4.2 over the 500 m west transect.

The opposite effects of the extreme clumping on L_e and Ω_E demonstrate the robustness of the optical methods when both LAI-2000 and TRAC are used. In other types of stands, such as jack pine and aspen where no such dense clumps exist, these optical methods are very reliable, as demonstrated in Figure 6.

5. Summary

Since direct measurements of LAI in forest stands are laborious and destructive in nature, our goal for future studies is to measure LAI using only optical instruments. Accurate optical measurements of LAI require consideration of canopy architecture at various scales. Measurement of the effective LAI *(L,)* is the first critical step in the optical measurements. LAI-2000 is very useful for this purpose and is recommended for future studies. Hemispherical photograph techniques are also useful for measuring L_e when the appropriate threshold values are selected to distinguish the foliage from the sky. L_e values measured in conifer stands were typically 50–70% direct estimates of LAI because of foliage clumping. The new optical instrument TRAC was able to measure the effect of foliage clumping at scales larger than the shoot, but the clumping within shoots must be estimated from shoot samples. The Sunfleck Ceptometer can be operated under the finite-length averaging principle to reduce the foliage clumping effect but cannot remove the small-scale clumping effect within the averaging length. With the fixed averaging length (0.8 m), the proportion of the clumping effect removed depends on the foliage element size and is not easily assessed. We therefore recommend the combined use of LAI-2000 (or hemispherical photography) and TRAC for future investigations. The LAI-2000 (or hemispherical photography) measures L_e without knowledge of the foliage angle distribution, and the TRAC measures Ω_E, which quantifies the effect of foliage spatial distribution on LAI measurements. These two parameters are combined (5) for the calculation of LAI. The other two parameters (α and γ_E) in (5) are less variable in mature boreal forests.

Allometric and optical results were in reasonable agreement for seven of the eight stands investigated. The difference between the results was 4% for SOJP, 10% for SYJP, 21% for NYJP, 9% in NOBS, 16% in NOJP, 34% in SOA, 36% in NOA, and 45% in SOBS. For the first five conifer stands, good agreement was found because the stands were relatively homogeneous at large scales and the difference in the optical and allometric measurement locations did not have a significant effect. For the two deciduous stands (SOA and NOA), the optical technique might have underestimated LAI because of (1) the inaccuracy in determining the clumping index due to the strong penumbra effect in the tall stands and (2) possibly the strong multiple scattering effect due to large leaf reflectance and transmittance. The worst case was found in SOBS, where tree density was highly variable. In SOBS the allometric plots and optical LAI transects were about 50-200 m apart, and therefore different LAI estimates were obtained. In addition to the spatial variability of LAI, allometric and optical results also contain considerable errors from different sources. In the allometric method, measurement errors in each step, such as leaf area/weight ratio, relationship between tree diameter and leaf area, and extrapolation from sample trees to plots and to the whole stand, etc., can accumulate, and it is difficult to keep the total error under 25%. In optical measurements there are three major sources of errors: (1) the measurement of clumping within shoots, (2) the effect of extreme foliage clumping, and (3) the estimation of contribution of woody materials. Each of these errors is in the range of 5–10%, making the sum of the error in the range of 15–30%. The error in optical results is therefore comparable to that in allometric results, and the validation of optical results by destructive sampling may not always be necessary if the accuracy requirement is about 75% of the true value. However, we do not exclude the possibility of much larger errors in optical results for stands with extreme architecture.

The measurements of LAI-2000 and TRAC are fairly easy and straightforward, but the major work load in making optical measurements of LAI is in obtaining the needle-to-shoot area ratio and woody-to-total area ratio. Nevertheless, these ratios are quite conservative in terms of their variability in mature stands. When quick LAI measurements are made with moderate accuracy requirements, constant values listed in Table 3 for these ratios can be used. The element clumping index measured by TRAC falls in the range 0.65-1.0, with most stands having values within 0.1 of 0.75 *[Chen and Cihlar*, 1996]. The typical values of this index are 0.65 (including the extreme clumping effect) for mature boreal black spruce and 0.75 for

iological Ecology: Field Methods and Instrumentation, edited by R. W. Pearcy et al., pp. 301-326, Chapman and Hall, New York, 1989.

Norman, J. M., and P. G. Jarvis, Photosynthesis in Sitka spruce (*Picea sitchensis* (Bong.) Carr.), III, Measurement of canopy structure and interception of radiation, J. *Appl. Ecol., 11, 375-398,* 1975.

Oker-Blom, P., Photosynthetic radiation regime and canopy structure in modeled forest stands, *Acta For. Fenn., 197,* l-44, 1986.

Pearcy, R. W., Radiation and light measurements, in *Plant Physiological Ecology: Field Methods and Instrumentation,* edited by R. W. Pearcy et al., pp. 95-116, Chapman and Hall, New York, 1989.

Rich, P. M., A manual for analysis of hemispherical canopy photography, *Los Alamos Natl. Lab. Rep., LA-11733-M,* 1989.

Rich, P. M., Characterizing plant canopies with hemispherical photographs, Instrumentation for studying vegetation canopies for remote sensing in optical and thermal infrared regions, *Remote Sens. Rev., 5,* 13-29, 1990.

Rich, P. M., D. A. Clark, D. B. Clark, and S. F. Oberbauer, Long-term study of solar radiation regimes in a tropical wet forest using quantum sensors and hemispherical photography, *Agric. For. Meteorol.,* 6.5, 107-127, 1993.

Rich, P. M., J. Chen, S. J. Sulatycki, R. Vashisht, and W. S. Wachspress, Calculation of leaf area index and other canopy indices from gap fraction: A manual for the LAICALC software, Open File Rep., Kans. Appl. Remote Sens. Progr., Lawrence, 1995.

Ross, J., The radiation regime and architecture of plant stands, Dr. W. Junk, Nor-well, Mass., 1981.

Ross, J., S. Kellomaki, P. Oker-Blom, V. Ross, and L. Vilikainen, Architecture of Scots pine crown: Phytometrical characteristics of needles and shoots, *Silva Fennica, 19,* 91-105, 1986.

Running, S. W., and J. C. Coughlan, A general model of forest ecosystem processes for regional applications, I, Hydrological balance, canopy gas exchange, and primary production processes, *Ecol. Modell., 42,* 125-154, 1988.

Sellers, P. J., Y. Mintz, Y. C. Sud, and A. Dalcher, A simple biosphere model (SiB) for use within general circulation models, J. *Atmos. Sci.,* 43, 505-531, 1986.

Stenberg, P., S. Linder, H. Smolander, and J. Flower-Ellis, Performance of the LAI-2000 plant canopy analyzer in estimating leaf area index of some Scots pine stands, *Tree Physiol., 14,* 981-995, 1994.

Vogel, J., Carbon and nitrogen dynamics of boreal jack pine stands with different understory vegetation, M.Sc. thesis, Univ. of Wisc., Madison, 1997.

Warren-Wilson, J., Stand structure and light penetration, I, Analysis by point quadrats, *J. Appl. Ecol., 2, 383-390,* 1965.

Welles, J. M., Some indirect methods of estimating canopy structure, *Remote Sens. Rev., 5,* 31-43, 1990.

J. M. Chen, Applications Division, Canada Centre for Remote Sensing, 419-588 Booth Street, Ottawa, Ontario, Canada K1A OY7. (e-mail: chen@ccrs.nrcan.gc.ca)

S. T. Gower, Department of Forestry, University of Wisconsin, 1630 Linden Drive, Madison, WI 53706.

J. M. Norman, Department of Soil Science, University of Wisconsin, 1525 Observatory Drive, Madison, WI 53706-1299.

S. Plummer, British National Space Centre, Abbots, Ripton, Huntingdon, Cambridgeshire, England PE172LS.

P. M. Rich, Department of Systematics and Ecology, Kansas Biological Survey and Environmental Studies Program, University of Kansas, Lawrence, KS 66045. (e-mail: prich@oz.kbs.ukans.edu)

(Received March 29, 1995; revised March 5, 1997;
accepted March 12, 1997.)